

A Pore Geometry Dependent Dispersion Model for the Dielectric Constant

M. T. Myers, Shell Exploration and Production Technology Company

Abstract

The effect of salinity, frequency and pore structure on the dielectric constant has been investigated for 28 carbonate samples. Laboratory measurements of the dielectric constant were performed between 1 MHz and 1.3 GHz. Two different measurement techniques were utilized, a coaxial technique and a parallel plate measurement. Measurements were performed at several salinities from .01 Molal to 1.0 Molal. Saturation measurements were also made on selected samples.

The measured dielectric constant is found to scale with the ratio of the measurement frequency to the conductivity of the saturating brine consistent with the dielectric dispersion mechanism attributed to a Maxwell-Wagner effect. The measured dispersion (frequency dependence) in the dielectric constant is dominated by two terms, proportional to the interparticle porosity and vuggy porosity respectively. The parameters in this model are consistent with earlier published models for the dielectric dispersion in clastics. At high salinities significant effects are present even at EPT* frequencies (1.3 GHz). An example is then given for applying this model to determine movable oil saturations from the EPT log in a vuggy carbonate.

Introduction

The EPT measures the dielectric constant of the formation at 1.1 GHz. This tool has a high vertical resolution (< 2 inches) and a shallow depth of investigation (1-2 inches). The most commonly used interpretation methods are the CRIM, CTA and TPO methods introduced by Schlumberger.^{1,2,3} Recent research suggests that the interpretation may be more complicated.^{4,5} Specifically, that pore geometry affects the dielectric dispersion and that the dispersion may be significant even at EPT frequencies. Similar to previous publications the dispersion in clean carbonates is attributed to the Maxwell-Wagner effect. This has two immediate implications, that the dispersion scales with the measured brine conductivity and that it is proportional to the volume fraction of the materials present.

These effects are present in the numerous EPT interpretation models that currently exist in the literature. These include Schlumbergers' CRIM, CTA, TPO, platy-grain model, and Exxons'

*Mark of Schlumberger

modified CTA model.^{1,2,3,6} CTA is the method commonly used in Schlumbergers' formation evaluation programs. The CRIM, CTA, and TPO models all assume the same mixing law for the rock matrix and fluid. They differ in the assumptions used to simplify the nonlinear mixing equation to determine the dielectric constants of the fluids and the matrix. In contrast, in the new pore geometry dependent dispersion model (PGDDM) the dispersion on the amounts of interparticle and vuggy porosity. Large amounts of vuggy porosity imply large dispersion. With the appropriate parameters a similarly large dispersion is predicted by the platy grain model, but as the name implies the dispersion was attributed to platy grains. This is contrary to laboratory measurements and point counts. Even in samples with large dispersion effects there were no platy grains found.

Salinity Dependence of the Dielectric Constant in Carbonates

The dielectric constant of 23 carbonate samples has been measured at several different salinities using the HP8505 network analyzer. The salinities were changed by placing the samples in brines of the appropriate salinity and allowing the samples to equilibrate by diffusion. Equilibrium was determined by monitoring the measured dielectric constant. The conductivities of the saturating brines were 1.21, 3.93, and 8.27 siemens/meter (6700, 24,100, and 54,400 ppm NaCl). These values of brine conductivity are representative of formation waters often found in carbonate reservoirs.

Figures one and two are typical examples of the salinity dependence of the dielectric constant and conductivities of a typical carbonate sample. The trend is that both the dielectric constant and the conductivity increase with salinity. Since these samples are clay free, interfacial polarization is expected to be the dominant mechanism causing the change in the dielectric constant. The dielectric constant will therefore scale with the ratio of the frequency to the conductivity of the saturating brine. This is because an interfacial polarization (the Maxwell-Wagner effect) is caused by the accumulation of charges on surfaces. The amount of charge that can contribute to this polarization mechanism will be proportional to the amount of charge and its mobility (determined by the conductivity) and will be limited by the amount

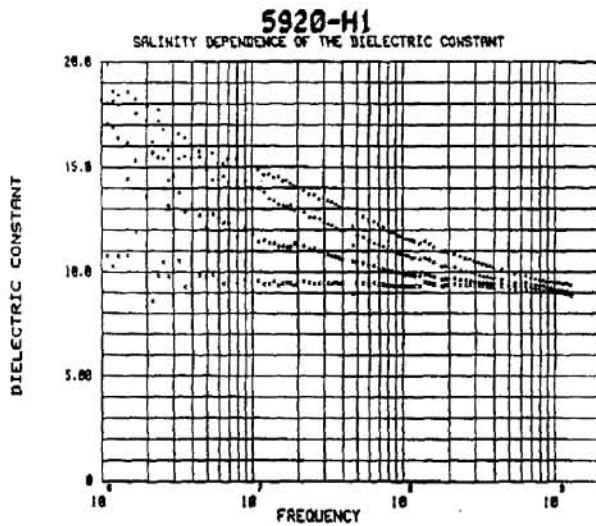


Figure 1. Salinity dependence of the dielectric constant for a carbonate sample.

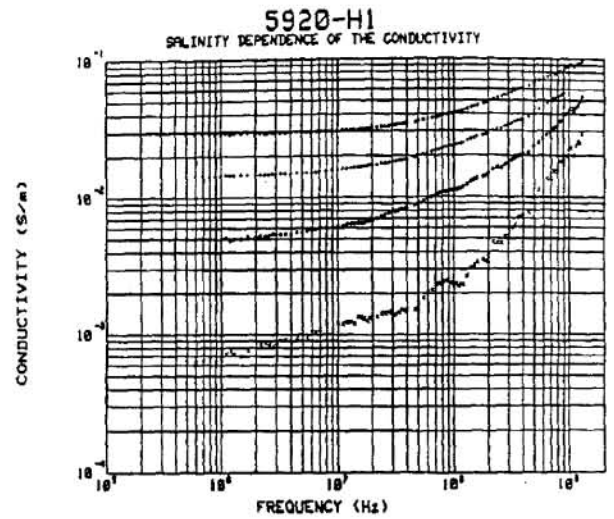


Figure 2. Conductivity measurement at 1.21, 3.93, 8.27 siemens/meter brines. Lowest conductivity is for distilled water.

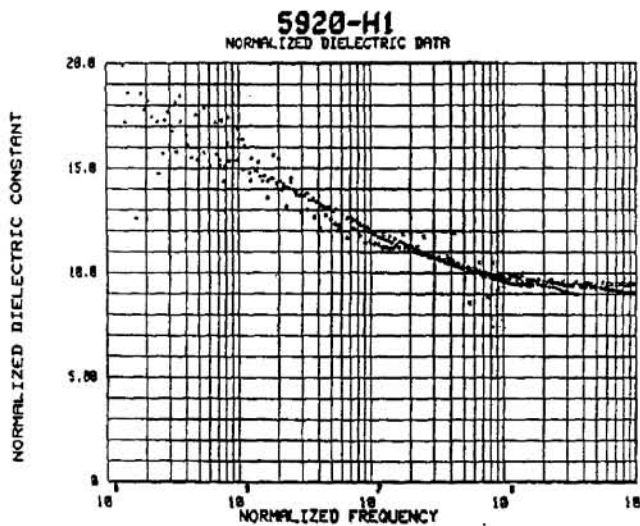


Figure 3. Dielectric constant plotted versus frequency normalized to brine conductivity.

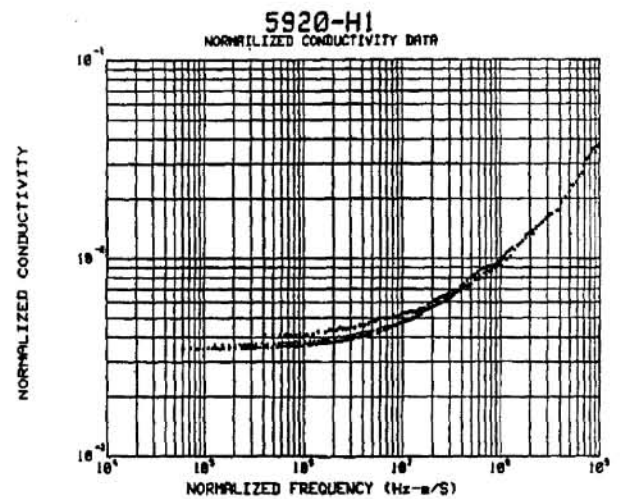


Figure 4. Normalized conductivity for 1.21, 3.93, and 8.27 siemens/meter brines.

of time these charges are allowed to move (inversely proportional to the frequency).

Figures three and four are the plots of the dielectric constant and conductivity data where the frequency has been normalized to the brine conductivity. The magnitude of the measured conductivity has also been normalized since it is also proportional to the brine conductivity (this is just the concept of a formation factor). To the accuracy of the data we find that both the dielectric constant and the measured conductivity scale with

the conductivity of the brine. The plots of all the data are of similar quality.

The scaling with brine conductivity implies that normalized curves can be defined which describe the frequency dependence of the dielectric constant and measured conductivity. To obtain the dielectric constant or sample conductivity from a normalized curve, it is simply shifted by an amount proportional to the brine conductivity. This is similar to the concept of a formation factor which is used for the low frequency conductivity. The measured data implies that a concept of a formation factor can be extended to higher frequencies and that we also can define an analogous brine conductivity normalized curve for the dielectric constant.

Similar experimental results have been reported at lower salinities in a single sample of Whitestone calcium carbonate.⁷ Our results, however, are based on a much larger sample set and at higher salinity, closer to those typically encountered in carbonate formations.

Comparison to the Dielectric Constant in Shaly Sands

In this section the effect of pore structure (i.e., the different effects of vuggy and inter-particle porosity) on the dielectric constant of carbonates is examined. The equation that has been previously proposed for the interpretation of the dielectric constant in clastics is:⁸

$$\epsilon = \epsilon_i * \phi + \epsilon_c * Q_{bv} + \epsilon_{hfl} \quad (1)$$

Where ϵ is the dielectric constant, ϵ_{hfl} is the limiting dielectric constant at high frequencies, ϵ_c is a fitted parameter giving the response due to clays, Q_{bv} is the cation exchange capacity normalized to the sample bulk volume and ϵ_i is the dielectric response due to the inter-particle porosity (ϕ) in these samples. Because the pore structure is more complicated in carbonates (e.g. vugs) an extra pore geometry term must be included. Since only carbonates that have small amounts of clays will be modeled, we will drop the clay term ($\epsilon_c \cdot Q_{bv}$) in Equation (1). This results in the following equation for the dielectric response of carbonates:

$$\epsilon = \epsilon_i * \phi_i + \epsilon_v * \phi_v + \epsilon_{hfl} \quad (2)$$

The terms ϵ_v and ϕ are fitted parameters which give the dielectric response due to the amount of vuggy porosity (ϕ_v) and the amount of inter-particle porosity (ϕ_i). We have measured the dielectric constant for 1 ohm-meter saturating brine for a set of 38 samples with a wide range in porosity (.4% to 42%) and fraction

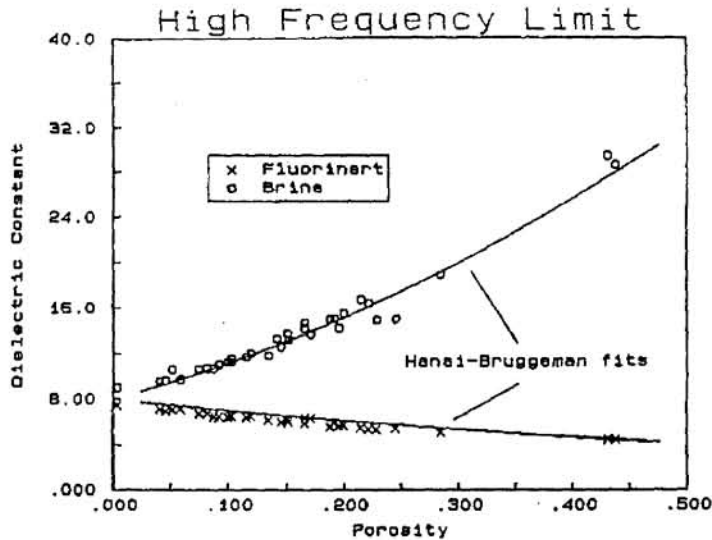


Figure 5. Measured high frequency limit for brine and fluorinert saturated samples. The solid lines are fits to the Hanai-Bruggeman equation. The distance between the two sets of data gives the magnitude of the saturation dependence. The scatter about either of the fits, related to the pore geometry, are small compared to the saturation dependence.

dielectric measurements with salinity the high frequency limit may be determined even at fairly low frequencies. The measured high frequency limit for brine and oil (fluorinert^{**}) saturated data are shown in Figure 5. This data can be fit to within experimental accuracies with a single pore geometry related parameter. This is in spite of the known wide variation in pore geometry in these samples (vugs versus inter-particle porosity). This implies that the pore geometry information in a high frequency limit measurement is quite small. Any pore geometry dependence will be in the dispersion of the dielectric constant. This is particularly evident when viewed in relation to the magnitude of the saturation dependence implied by this data (given by the distance between the two sets of data).

Pore Geometry Terms ϵ_i and ϵ_v

The fitted porosity terms ϵ_i and ϵ_v are shown in Figure 2. The vuggy and inter-particle porosities for the samples were determined using the measured low frequency conductivity, total porosity and a model for the low frequency conductivity. This model is provided in a previously published paper for the conductivity in formations with multiple pore systems. The expression for the formation factor is:

of vuggy porosity (0% to >70%). We will discuss the results of the fit of Equation(2) to these data in the rest of this paper.

The High Frequency Limit Term

The high frequency limit, ϵ_{hfl} , was calculated from the Hanai-Bruggeman equation.^{9,10} Use of this equation to model the high frequency limit of the dielectric constant and the low frequency limit of the conductivity has been discussed in detail in previous papers^{11,12}. We obtain high frequency limit data from low salinity measurements (.01 molal) of the dielectric constant. Because of the scaling of

^{**}Trademark of 3M Corporation

$$F = (1/\phi_i)^{1.91} * (\phi_i/\phi)^{1.16} \quad (3)$$

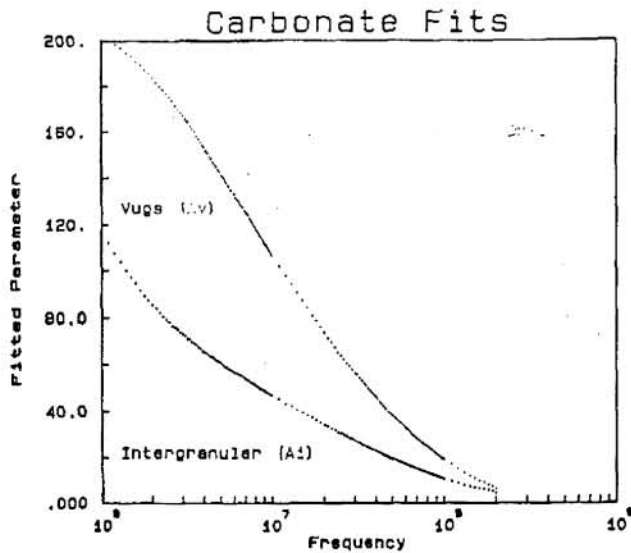


Figure 6. The fitted vug (ϵ_v) and intergranular (ϵ_i) terms for 1 ohm-meter brine. The fits imply that the dielectric dispersion increases faster with vuggy porosity than intergranular porosity.

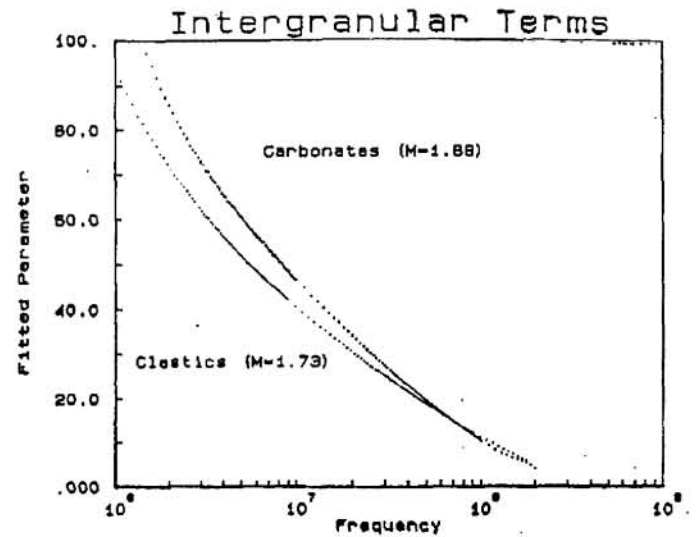


Figure 7. Comparison of the interparticle terms for carbonates and clastics.

Where again ϕ is the total formation porosity (interparticle and vuggy) and ϕ_i is the inter-particle porosity alone. The details of this procedure, as well as methods to obtain a low frequency conductivity from dielectric measurements, will be published elsewhere. For comparison we have shown the intergranular term from the clastic fits in Figure(3). The two fits are within error bars of each other with the carbonate term being slightly larger. The average Archie m values for these pore systems are also shown. These values suggest that there may be a slight dependence of the dielectric dispersion on m . The agreement between the fitted values for the carbonate and clastic inter-particle terms is strong evidence supporting the validity of Equation (2) and the interpretation of the terms.

In Figures 8 and 9 we show the comparison at this salinity between the measured and fitted values for 25 MHz and 200 MHz data. The agreement is quite good with an average error of about two dielectric units.

We can use Equation(2) and Figure(1) to determine inter-particle and vuggy porosity over a wide range of salinities and frequencies. To do this we make use of the scaling of the measurements with brine conductivity. This scaling means that there is a trade-off between the measurement frequency and the

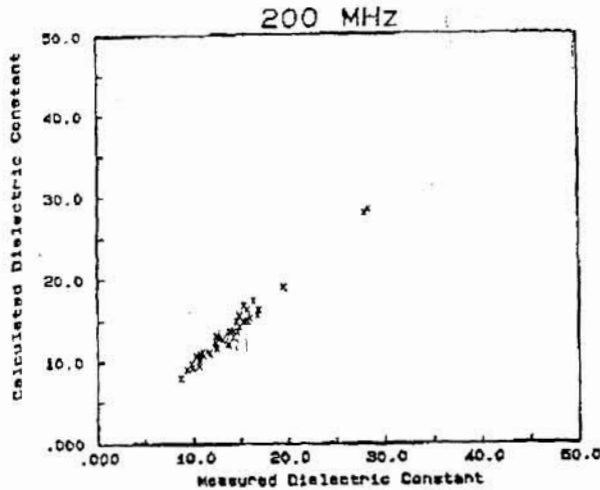


Figure 8. The measured versus the calculated dielectric constant at 200 MHz.

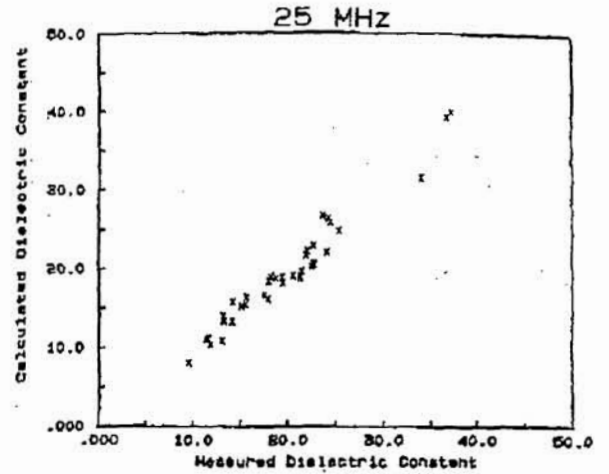


Figure 9. The measured dielectric constant at 25 MHz compared to the calculated value.

resistivity of the saturating brine. The values of ϵ_i and ϵ_v may be read from Figure 1 at the measurement frequency for rocks containing 1 ohm-meter brines. For saturating brines with different resistivities multiply the measurement frequency by the brine resistivity and enter at this new value. For example, at 20 MHz and a brine resistivity of .1 ohm-meters you enter at, 20 MHz * .1 = 2 MHz, and read the values of ϵ_i and ϵ_v from the chart. Knowing the measured dielectric constant and total porosity it is a simple matter to solve Equation (2) for the inter-particle and vuggy porosity. If the brine resistivity is unknown the above procedure can be iterated until the estimate of the vuggy and

inter-particle porosity using the conductivity to interpret the conductivity and the dielectric constant agree.

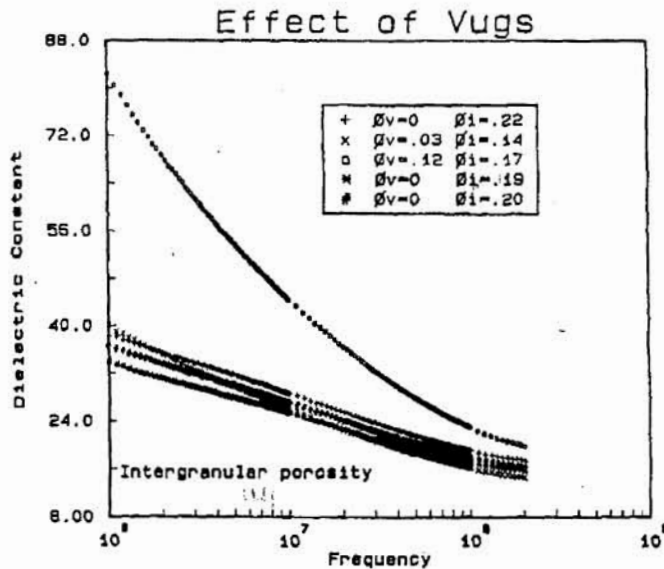


Figure 10. The dielectric response of several samples from the same formation. The samples with the lowest interparticle porosity have the largest amount of dispersion because they also contain the largest vuggy porosity.

An example of the Dielectric Response of Vugs

As has been shown in Figure(2) the dielectric response for vugs and inter-particle porosity is quite different, with the vuggy porosity contributing more to the dispersion than the inter-particle porosity. This effect is illustrated for individual samples in Figure(6) where we have plotted the measured

dielectric data for several carbonate samples from New Mexico. The dramatic difference in the dielectric dispersion for the one sample is due to the high vug content (12 percent ϕ_v , 17 percent ϕ) as compared to the four other samples which are all about 20 percent inter-particle porosity.

Measuring movable oil saturations with the EPT

Since the EPT only measures in the flushed zone, the EPT needs to be corrected for dispersion effects using equations (1) and (2) when wells are drilled with high salinity drilling fluids. Since the dispersion also depends on pore geometry we need another equation to determine the saturation. We again use equation (3) to determine the vuggy and interparticle porosity for the conductivity. Assuming the MSFL (Micro Spherically Focused Log) sees the same flushed zone as the EPT we can solve equations (1) and (3) for the flushed zone oil saturation. If combined with the formation water saturation obtained from a deep resistivity log, a movable oil saturation can also be determined.

An example for determining movable oil saturations is displayed in figure (11). Track (2) of the log suite contains the calculated deep and shallow water saturations. The deep water saturation was calculated using the deep Dual Laterolog (DLL) and the shallow residual oil saturation using the EPT. High oil saturations were measured using both techniques and shallow techniques implying low movable oil volumes. This and other examples are given in more detail in a previous publication.¹³

Conclusions

We have shown that to the accuracy of our data that the dielectric constant scales with the conductivity of the saturating brine. This is strong experimental evidence that pore structure effects are dominating the dielectric response of these samples, (in shaly sands this scaling did not exist). This is an important step toward determining a brine saturated mixing law for carbonates. Since the pore structure is also important in determining the permeability of carbonate reservoirs, dielectric measurements may some day prove useful for estimating permeability using dielectric log data.

The interpretation of the EPT in high salinity environments is affected by dielectric dispersion. In carbonates, the dispersion is a function of pore geometry (vuggy versus inter-particle porosity). The widely used interpretation methods such as CRIM, CTA, and TPO do not properly include these effects and will therefore include significant errors in the calculated saturations. Using EPT log data the pore geometry effects measured in the laboratory can be quantitatively confirmed in 100% water saturated zones. This dispersion model if used with a variable Archie

exponent model allows an accurate calculation of residual and movable oil saturations in complicated lithologies.

References

1. Calvert, T.J. et. al.: Electromagnetic Propagation ... A New Dimension in Logging, SPE 6542 (1977)
2. Wharton, R.P. et.al.: Electromagnetic Propagation Logging: Advances in Technique and Interpretation, SPE 9267 (1980).
3. Dahlberg, K.E. and Ference, M.V.; A Quantitative Test of the Electromagnetic Propagation (EPT) Log for Residual Oil Determination, SPWLA Twenty-Fifth Annual Logging Symposium, (June 10-13, 1984).
4. Kenyon, W.E. and Baker, P.L.: EPT Interpretation in Carbonates Drilled with Salt Muds, SPE 13192 (1984).
5. Chang, D. and Myers, M.T.: Estimation of Producible and Remaining Oil Using High Frequency Dielectric Logs in Carbonate Reservoirs, SPE 30586 (1995)
6. Kenyon, W.E. and Baker, P.L.: EPT Interpretation Using a Textural Model, SPWLA Twenty-Sixth Annual Logging Symposium, (June 17-20, 1985)
7. Kenyon, W.E., Texture Effects on Megahertz Dielectric Properties of Calcite Rock Samples, J. Appl. Phys. 55(8), pp. 3153-3159, April (1984).
8. Myers, M.T.: A Saturation Interpretation Model for the Dielectric Constant of Shaly Sands, SCA (1991).
9. Hanai, T., Electrical Properties of Emulsions, Chapter 5 in Emulsion Science, Academic Press (1968).
10. Bruggeman, von D.A.G.: , Berechnung Verschiedener Physikalischer Konstanten von Heterogenen Substanzen, Ann. Phys. Lpz. Vol.24 pp. 636 (1935).
11. Myers, M.T.: A Saturation Interpretation Model for the Dielectric Constant of Shaly Sands, SCA (1991).
12. Myers, M.T.: Pore Combination Modeling: Extending the Hanai-Bruggeman Equation, SPWLA (1989)
13. Chang, D. and Myers, M.T.: Estimation of Producible and Remaining Oil Using High Frequency Dielectric Logs in Carbonate Reservoirs, SPE 30586 (1995)

